Immunology
The Journal of cells, molecules, systems and technologies

British Society for immunology

IMMUNOLOGY ORIGINAL ARTICLE

Ablation of the cellular prion protein, PrP^C, specifically on follicular dendritic cells has no effect on their maturation or function

Laura McCulloch, Karen L. Brown and Neil A. Mabbott

The Roslin Institute and Royal (Dick) School of Veterinary Sciences, University of Edinburgh, Midlothian, UK

doi:10.1111/imm.12031
Received 27 July 2012; revised 19 October 2012; accepted 22 October 2012.
Correspondence: Neil A. Mabbott, The Roslin Institute and Royal (Dick) School of Veterinary Sciences, University of Edinburgh, Easter Bush, Midlothian EH25 9RG, UK. E-mail: neil.mabbott@roslin.ed.ac.uk
Senior author: Neil A. Mabbott

Summary

Follicular dendritic cells (FDC) are situated in the primary follicles of lymphoid tissues where they maintain the structural integrity of the B-lymphocyte follicle, and help to drive immunoglobulin class-switch recombination, somatic hypermutation and affinity maturation during the germinal centre response. FDC can also provide a reservoir for pathogens that infect germinal centres including HIV and prions. FDC express high levels of the normal cellular form of the prion protein (PrP^C), which makes them susceptible to prion infection. The function of PrP^C is uncertain and it is not known why FDC require such high levels of expression of a protein that is found mainly on cells of the central nervous system. In this study, the function of FDC was assessed in mice that had PrP^C ablated specifically in their FDC. In mice with FDC-specific PrP^C ablation, our analysis revealed no observable deficits in lymphoid follicle microarchitecture and FDC status. No effects on FDC ability to trap immune complexes or drive antigen-specific antibody responses and affinity maturation in B lymphocytes were observed. These data clearly demonstrate that PrP^C expression is dispensable for the functional maturation of FDC and their ability to maintain antigen-specific antibody responses and affinity maturation.

Keywords: antibody response; follicular dendritic cell; germinal centre; prion protein; spleen.

Introduction

Follicular dendritic cells (FDC) are a non-migratory, non-phagocytic stromal cell population found in the B-lymphocyte follicles of secondary lymphoid tissue. They form networks of long dendrites, which enable close contact with many B lymphocytes and help to maintain the structural integrity of the follicle.[1] Furthermore, FDC secrete the chemokine CXCL13, which stimulates the chemotaxis of further CXCR5-expressing B lymphocytes into the follicle.[2] The FDC are thought to derive from a stromal cell precursor[3,4] that develops after the arrival of B lymphocytes into the follicle[5] and their induction and maintenance is dependent on B-lymphocyte-derived lymphotoxin and tumour necrosis factor-α.[6,7] They have recently been shown to develop from precursors that are found around blood vessels, and require lymphoid tissue inducer cells and lymphotoxin for their expansion. These characteristics allow the development of FDC-containing ectopic lymphoid follicles outwith the lymphoid tissues during chronic inflammatory conditions.[8]

In addition to the development and maintenance of the follicle microarchitecture, FDC are also important in driving the germinal centre (GC) response. The FDC express complement receptors (CR1, CR2 and possibly CR3) and immunoglobulin Fc receptors (FcγRIIb and possibly FcεRII), which allow them to capture antigen in the form of immune complexes.[5,9] Antigens are retained on FDC surfaces in their native states for long periods of time to aid the positive selection of high-affinity B lymphocytes during the GC response.[1,7,10–14] FDC further aid this process by up-regulating the expression of adhesion

Abbreviations: AP alkaline phosphatase; CR complement receptor; DNP-KLH dinitrophenyl–keyhole limpet haemocyanin; FDC follicular dendritic cell; GC germinal centre; ICAM intercellular adhesion molecule; mAb monoclonal antibody; PAP peroxidase–anti-peroxidase; PrP^C cellular isomer of the prion protein; TCR T-cell receptor; TLR Toll-like receptor; VCAM vascular cell adhesion molecule; WT wild-type

molecules such as intercellular adhesion molecule (ICAM), vascular cell adhesion molecule (VCAM) and CD44 to facilitate interactions between B lymphocytes and the retained antigen on the FDC surface.[1,12,15,16] The competitive binding to antigen on the FDC surface allows B lymphocytes with the highest affinity for the eliciting antigen to receive pro-survival signals from FDC via B-cell activating factor and 8D6 signalling and cytokines such as interleukin-6 and interleukin-15.[17–20] FDC can also target low-affinity B lymphocytes for apoptosis via their secretion of milk fat globule EGF factor 8.[21]

Surface proteins of FDC are also exploited by certain pathogens. This results in a reservoir of pathogen in the GC that can then spread systemically via other cells trafficking through the lymphoid tissue. For example, HIV uses CD21 expression on FDC to become trapped on their surfaces where it is then able to replicate and infect B lymphocytes.[22] Prions comprise a unique group of pathogens thought to be composed solely of protein with no genetic material. Infection with prions is considered to induce a conformational change in the normal host prion protein (PrP^{C}) to an abnormally folded, infectious form (PrP^{Sc}). Furthermore, expression of PrP^{C} is essential for prion pathogenesis to occur.[23] After peripheral exposure to some prion diseases, FDC acquire PrP^{Sc} and replicate prions, which allows subsequent neuroinvasion and fatal central nervous system disease.[24,25] FDC are susceptible to infection by prions because of their expression of relatively high levels of PrP^{C} on their surfaces.[24,25]

The cellular isomer of the prion protein is a host-encoded sialoglycoprotein (encoded by the *Prnp* gene in mice), which is expressed predominantly on neurons but also on many other cell types, including cells of the immune system.[26–29] The normal cellular function of PrP^{C} is uncertain and three independent lines of *Prnp*$^{-/-}$ mice show normal development and have no overt neurological phenotype, suggesting that either PrP^{C} is not an essential protein or that genetic loss of PrP^{C} can be compensated for by other mechanisms.[23,30–32] Some proposed functions of PrP^{C} include the maintenance of circadian rhythm,[33] synaptic transmission,[34] anxiety modulation,[35] cognition[36] and seizure thresholds[37] as small changes in these functions have been observed in *Prnp*$^{-/-}$ mice. PrP^{C} has also been proposed as a signal transduction protein[38,39] and has been suggested to have roles in both pro-apoptotic signalling via an associated increase in caspase 3 activity,[40] and anti-apoptotic activity via binding to the anti-apoptotic molecule Bcl-2.[41,42] Furthermore, PrP^{C} expression has been reported to protect both cells of the central nervous system and those of the immune system from oxidative stress.[43,44] The role of PrP^{C} on FDC is uncertain. Therefore, in this study, mice which had PrP^{C} expression ablated exclusively on FDC were used to determine the role of PrP^{C} in the FDC status and the development of antigen-specific antibody responses.

Materials and methods

Mice

The CD21-Cre mice[45] and *Prnp*$^{flox/flox}$ mice[46] were generated as described previously. Each had been inbred for at least 10 generations before being bred and maintained on a *Prnp*$^{-/-}$ background.[47] *Prnp*$^{flox/flox}$ mice have *loxP* sites flanking exon 3 of the *Prnp* gene, which enables Cre-mediated excision of the *Prnp* open reading frame in Cre-recombinase-expressing cells.[46] To create *CD21-CrePrnp*$^{flox/-}$ mice a single cross between the CD21-cre mice and the *Prnp*$^{flox/flox}$ mice was performed. All mice were maintained under specific pathogen-free conditions. All studies using experimental mice and regulatory licences were approved by the University of Edinburgh's Ethics Review Committee and performed under the authority of a UK Home Office Project Licence within the regulations of the UK Home Office 'Animals (scientific procedures) Act 1986'.

γ-irradiation and bone marrow reconstitution

Bone marrow from the femurs and tibias of donor mice was prepared as single-cell suspensions (3×10^7 to 4×10^7 viable cells/ml) in Hanks' balanced salt solution (Invitrogen, Paisley, UK). Recipient adult (6–8 weeks old) mice were γ-irradiated (950 rad) and 24 hr later were reconstituted with 100 μl bone marrow by injection into the tail vein. Recipient mice were used in subsequent experiments as described, 100 days after bone marrow reconstitution to allow sufficient time for the removal of long-lived B-lymphocyte populations and their replacement from the donor bone marrow.

Confirmation of recombination of the Prnp *open reading frame by PCR analysis*

DNA was prepared from peripheral blood and spleens of bone marrow-reconstituted *CD21-CrePrnp*$^{flox/-}$ mice using the DNeasy blood and tissue kit (Qiagen, Crawley, UK) according to the manufacturer's instructions. DNA samples were analysed for the presence of *Prnp*$^{-/-}$, *Prnp*^{flox} and recombined *Prnp*^{flox} (*Prnp*$^{de\text{-}flox}$) using the following primers: *Prnp*^{flox} Primer 1, AATGGTTAAACT TTCGTTAAGGAT; *Prnp*^{flox} Primer 2, GCCGACATCA GTCCACATAG; *Prnp*^{flox} Primer 3, GGTTGACGCCAT GACTTTC. The PCR products were resolved by electrophoresis through a 1·0% agarose gel containing 0·002% GelRed (Biotium; Cambridge Biosciences Ltd, Cambridge, UK). Presence of *Prnp*$^{-/-}$ is indicated by a 167-bp product, *Prnp*^{flox} by a 210-bp product and *Prnp*$^{de\text{-}flox}$ by a 344-bp product.

Immunohistochemistry and immunofluorescent analyses

Spleens were removed and snap-frozen in liquid nitrogen. Serial frozen sections (8 μm in thickness) were cut on a cryostat and immunostained with the following antibodies: FDC were visualized by staining with monoclonal antibody (mAb) 7G6 to detect CR2/CR1 (CD21/CD35; BD Biosciences PharMingen, Oxford, UK), mAb FDC-M2 to detect C4 (AMS Biotechnology, Oxon, UK) or mAb 8C12 to detect CR1 (CD35; BD Biosciences PharMingen). PrP^C was detected using the PrP-specific 1B3 polyclonal antiserum.[48] B cells were detected using mAb B220 to detect CD45R (Caltag, Towcester, UK), or anti-CD19 (BD Biosciences PharMingen). Marginal zone B cells were detected using mAb 1B1 to detect CD1d (BD Biosciences PharMingen). T cells were detected using mAb 17A2 to detect CD3 (Cambridge Bioscience). Classical dendritic cells were detected using mAb HL3 to detect CD11c (BD Biosciences PharMingen). Mucosal vascular addressin cell adhesion molecule (MADCAM) 1-expressing cells were detected using mAb MECA-367 (AbD Serotec, Kidlington, UK). Expression of VCAM was detected using mAb STA to detect CD106 (Caltag). Toll-like receptor 4 (TLR4) expression was detected using mAb 76B357.1 (Abcam, Cambridge, UK). Splenic sympathetic nerves were detected using tyrosine hydroxylase-specific polyclonal antibody (Millipore, Watford, UK).

For light microscopy, following the addition of primary antibodies, biotin-conjugated species-specific secondary antibodies (Stratech, Soham, UK) were applied followed by alkaline phosphatase (AP) coupled to the avidin/biotin complex (Vector Laboratories, Peterborough, UK). Vector Red (Vector Laboratories) was used as a substrate and sections were counterstained with haematoxylin to distinguish cell nuclei. Sections were mounted in Vectamount (Vector Laboratories) and examined using a Nikon Eclipse E800 microscope (Nikon UK Ltd, Surrey, UK). For fluorescent microscopy, following the addition of primary antibody, species-specific secondary antibodies coupled to Alexa Fluor® 488 (green), Alexa Fluor® 594 (red) or Alexa Fluor® 647 (blue) dyes (Invitrogen) were used. Sections were mounted in fluorescent mounting medium (DakoCytomation) and examined using a Zeiss LSM5 confocal microscope (Zeiss, Welwyn Garden City, UK).

Image analysis

Digital microscopy images were analysed using IMAGEJ software (http://rsb.info.nih.gov/ij/) as described.[49] All images were coded and assessed blindly. Background intensity thresholds were first applied using an IMAGEJ macro that measures pixel intensity across all immunostained and non-stained areas of the images. The obtained pixel intensity threshold value was then applied in all subsequent analyses. Next, the number of pixels of each colour (black, red, green, yellow) was automatically counted and presented as a proportion of the total number of pixels in each area under analysis. Analysis of positive labelling was used to determine the area of FDC network immunostained in each section. Spleens from six mice from each group were analysed. From each spleen, two sections were studied and on each section data from four randomly chosen fields of view over the entire section were collected. Hence, for each mouse group, data from a total of 48 individual images were analysed. To compare the number of FDC networks, the number of CD35-immunolabelled FDC networks in two sections from each spleen from each mouse ($n = 6$) in each group were studied. On each of these sections the number of $CD35^+$ FDC networks was counted in each of four randomly chosen fields of view when viewed with the $\times 10$ objective. Hence, for each parameter tested, data from a total of 48 individual images/FDC networks were analysed/group. A one-way analysis of variance test was then used to statistically compare data between each group.

FACS analysis

Single spleen cell suspensions were prepared and red blood cells were removed using red blood cell lysis buffer (Sigma, Poole, UK). Viable cells were counted by trypan blue-exlusion and adjusted to 1×10^6 viable cells/50 μl in FACS buffer (PBS pH7·4 containing 0·1% BSA, 0·1% sodium azide and 0·02% EDTA). Non-specific immunoglobulin-binding was blocked using Seroblock FcR rat anti-mouse CD16/32 (AbD Serotech, Kidlington, UK) and subsequently immunostained with mAb 7G6 to detect CD21/35 and PrP-specific 1B3 polyclonal antiserum. Samples were then incubated with phycoerythrin-conjugated and FITC-conjugated species-specific secondary antibodies. Appropriate non-specific antibody isotypes were used as controls. A FACS Scan flow cytometer (Becton Dickinson, Oxford, UK) was used to analyse cells with the lymphocytes gated for forward and side scatter.

Immunizations

To assess antigen trapping by FDC *in vivo*, mice were passively immunized by intravenous injection with 100 μl pre-formed peroxidase–anti-peroxidase (PAP) immune complexes (Sigma). Spleens were removed 24 hr later and the presence of FDC-associated immune complexes was identified by both immunohistochemistry and detection of peroxidase activity using the substrate Novared (Vector Laboratories).

To assess the ability of FDCs to induce an effective antigen-specific B-lymphocyte response, mice were immunized on day 0 intraperitoneally with 100 μl of 1 μg/μl dinitrophenyl–keyhole limpet haemocyanin (DNP-KLH)

in alum and given a boost with an equivalent intraperitoneal dose on day 14. Tail bleeds were taken on days 0 and 7, and mice were killed on day 21 and blood and spleens were harvested for further analysis.

ELISA for DNP-specific serum antibodies

Sera from immunized mice were assayed using DNP-specific ELISAs for IgM, total IgG and IgG subclasses. In brief, 96-well flat-bottomed Immuno-Maxisorp plates (Nunc, Roskilde, Denmark) were coated by adding 100 μl/well of 10 μg/μl DNP-BSA (Sigma) in PBS (pH 7·6) overnight at 4°. Plates were washed with PBS containing 0·05% Tween 20 (PBS-Tween) and blocked with 1% BSA in PBS for 1 hr. Serum samples were diluted in block buffer (1% BSA in PBS), added in duplicate wells and incubated for 2 hr. For the determination of IgM antibodies, samples were incubated with AP-conjugated goat anti-mouse IgM (1/2000 dilution in PBS containing 1% BSA; Southern Biotech, Birmingham, AL) for 1 hr at room temperature. For measuring total IgG antibodies, samples were incubated with an AP-conjugated goat anti-mouse IgG Fc region antibody (1/2000; Southern Biotech). For the determination of IgG1, IgG2a, IgG2b and IgG3 antibody subclasses, plates were incubated with peroxidase-labelled goat anti-mouse IgG subclass-specific antibodies (1 : 2000; Southern Biotech). All ELISAs were developed with Sigmafast *p*-nitrophenyl phosphate (Sigma) and optical density at 640 nm was measured using an MRX microplate Reader (Dynatech Labs, Chantilly, VA).

Statistical analyses

Data are presented as mean ± SE. Significant differences between image analysis samples in different groups were sought by one-way analysis of variance. Significant differences between sera ELISA samples in different groups were sought by Bonferonni analysis using the SPSS statistical analysis software package (SPSS Inc., Chicago, IL). Values of $P < 0{\cdot}05$ were accepted as significant.

Results

Creation of compound transgenic mice with PrP^C ablation specifically restricted to FDC

To achieve PrP^C ablation specifically in FDC, *CD21-CrePrnp$^{flox/-}$* mice were created as described in the Materials and Methods. In these mice, Cre-recombinase is expressed under the control of the CD21 promoter, which in the secondary lymphoid organs of mice is highly expressed by FDC and mature B lymphocytes.[50,51] However, in humans, expression of CD21 has also been reported on a subpopulation of immature thymocytes,[52] peripheral T lymphocytes[53] and the cervical epithelium.[54] In mouse, expression has been reported on mesenteric lymph node-derived CD4$^+$ T lymphocytes, activated granulocytes and mucosal mast cells.[10,11,55] Therefore, to achieve Cre-mediated excision of the *Prnp* open reading frame specifically in FDC, *CD21-CrePrnp$^{flox/-}$* animals were aged to 8 weeks, lethally γ-irradiated and reconstituted with non-*Cre*-expressing bone marrow. Animals were given 100 days for reconstitution before further experimental analysis was carried out. Previous characterization of this model has shown it to be a specific and efficient model to achieve gene deletion specifically in FDC.[2,7,25] PCR analysis of DNA isolated from the spleens of *CD21-CrePrnp$^{flox/-}$* mice revealed that Cre-mediated DNA recombination (deletion or *de-flox*) of the *Prnp* gene had occurred as anticipated, indicating that PrP^C expression was ablated in the host-derived, FDC-containing stromal compartment of the spleen (Fig. 1a; presence of 344 bp '*Prnp*$^{de\text{-}flox}$' band, lane 2). In contrast, no evidence of Cre-mediated DNA recombination of the *Prnp* gene was detected in the peripheral blood of the *CD21-CrePrnp$^{flox/-}$* mice indicating that PrP^C expression was not affected in the haematopoietic compartment (including lymphocytes) of these mice (Fig. 1a; presence of the 210-bp '*Prnp*^{flox}' band and absence of '*Prnp*$^{de\text{-}flox}$' band, lane 1). Further analysis of splenic CD21$^+$ B lymphocytes by FACS showed similar, low levels of PrP^C on cells from wild-type (WT) mice and *CD21-CrePrnp$^{flox/-}$* mice (Fig. 1b). Together, these data demonstrate that efficient Cre-mediated ablation of the *Prnp* gene had occurred in the FDC, but not B lymphocytes, of bone marrow-reconstituted *CD21-CrePrnp$^{flox/-}$* mice. Immunohistochemical analysis of spleens from WT mice confirmed high levels of PrP^C labelling on FDC networks (Fig. 1c, top panels). In contrast, FDC in spleens from *CD21-CrePrnp$^{flox/-}$* mice lacked PrP^C expression, confirming that Cre-mediated excision of the *Prnp* open reading frame had occurred (Fig. 1c, bottom panels). In addition to FDC, high levels of PrP^C expression were also observed upon tyrosine hydroxylase$^+$ sympathetic nerves in the spleens of WT control mice (Fig. 1d, upper panel). In the spleens of *CD21-CrePrnp$^{flox/-}$* mice, high levels of PrP^C expression were also observed upon splenic nerves (Fig. 1d, lower panel). Morphometric analysis confirmed that the magnitude of the PrP^C expression co-localized upon the surfaces of tyrosine hydroxylase$^+$ sympathetic nerves in the spleens of *CD21-Cre Prnp$^{flox/-}$* mice was not significantly different when compared with controls (Fig. 1e, open bars, $P = 0{\cdot}390$). In contrast, the magnitude of the PrP^C expression co-localized upon the surfaces of FDC in the spleens of *CD21-Cre Prnp$^{flox/-}$* mice was substantially and significantly lower than that observed upon FDC from control mice (Fig. 1e, closed bars, $P < 1{\cdot}0 \times 10^{-22}$). Taken together, these data confirm that in the spleens of the bone marrow-reconstituted CD21-Cre

Prnp$^{flox/-}$ mice the *Prnp* ablation was specifically restricted to FDC.

PrP^C expression by FDC has no role in FDC-mediated organization of the lymphoid follicle

To understand the effects of PrP^C ablation on FDC-dependent organization of the B-lymphocyte follicle, lymphoid tissue microarchitecture was assessed in spleens from mice with PrP^C ablation specifically restricted to FDC and compared with tissues from WT and single transgenic controls. The FDC were immunolabelled with a variety of commonly used markers: CD21/35 (CR2/CR1) and complement component C4. Each of these showed no observable difference in their distribution in spleens from mice from each group (Fig. 2a). Similarly there were no apparent differences in the distribution of B and T lymphocytes and CD11c$^+$ classical dendritic cells between the mouse lines (Fig. 2a). Additionally, no disruptions to the microarchitecture of the B-lymphocyte follicles, T-cell zones and marginal zones were noted (Fig 2a). In contrast to B cells, FDC in mice specifically express high levels of CD35 (CR1) (Fig. 2b). We therefore used anti-CD35 immunolabelling to measure the number and area of FDC networks in spleens from each group of mice. No significant differences in the number or area of FDC networks in the spleen were found between mice with PrP^C ablation specifically in FDC and controls (Fig. 2c). These data show that FDC-specific PrP^C ablation had no observable effect on the organization of the lymphoid tissue microarchitecture. These data suggest that PrP^C on FDC does not have a role in the ability of these cells to induce and organize the development of the follicle structure.

Ablation of PrP^C specifically in FDC has no effect on their ability to trap and retain immune complexes

The FDC's ability to trap and retain native antigen in the form of immune complexes is important for the development of effective humoral immune responses.[10,12,56] The distribution, but not the amount, of antigen on the FDC surface and the stoichiometry of antibody : antigen interactions can affect the avidity of downstream humoral immune responses.[57–59] As PrP^C is found in membrane lipid rafts, it was hypothesized that the ablation of PrP^C on the FDC surface may change the organization of surface membrane proteins, and indirectly, affect the ability of the FDC to initiate an efficient humoral immune response. The ability of FDC to trap and retain antigen *in vivo* was assessed by injecting pre-formed PAP immune complexes. The retention of the PAP immune complexes on the FDC network was determined by the histological assessment of the association of peroxidase activity or rabbit immunoglobulin from the PAP complexes with FDC (CD35-expressing cells). No differences were apparent in either the levels of peroxidase activity (Fig. 3a, upper panels) or the amount of rabbit immunoglobulin (Fig. 3a, lower panels) bound to the surfaces of FDC from mice from each group. Furthermore, morphometric analysis confirmed that no significant difference was observed in the mean number of PAP$^+$ pixels detected on FDC networks in mice from each group (Fig. 3b, $P = 0{\cdot}977$). These data show that FDC do not require the expression of PrP^C to trap and retain immune complexes on their surfaces.

PrP^C expression by FDC is dispensable for the induction of antigen-specific antibody production and affinity maturation

We next determined whether the ablation of PrP^C in FDC affected their ability to support B-lymphocyte generation of high-affinity, class-switched immunoglobulin. Mice from each group were immunized with DNP-KLH and serum levels of antigen-specific immunoglobulin levels were compared. Seven days after primary immunization the titres of antigen-specific IgM (Fig. 4a, $P = 1$) or total IgG (Fig. 4c, $P > 0{\cdot}07$) detected in the sera were not significantly different between all of the mouse groups tested. This suggests that ablation of PrP^C on FDC has no impact on the ability of the FDC to support an efficient primary antibody response within the germinal centre. At day 21 (7 days after booster immunization) mice with PrP^C ablated on FDC showed significantly lower titres of IgM in comparison to WT controls (Fig 4b, $P < 0{\cdot}001$). However, single transgenic control groups also had similarly reduced titres of IgM and therefore this reduction cannot be attributed to the loss of PrP^C on the FDC and is more likely a result of subtle differences in the host genetic background. Titres of total antigen-specific IgG at day 21 showed no significant differences between groups (Fig. 4d, $P > 0{\cdot}07$). These data suggest that the ablation of PrP^C in FDC does not significantly impact the efficiency of the germinal centre to support a secondary antibody response in immunized animals.

Serum levels of IgG subclasses were also compared to assess if mice with PrP^C ablated on FDC showed any impairment in affinity maturation via the ability to class switch their immunoglobulin. Mice with PrP^C ablation on FDC had significantly higher titres of IgG1 (Fig. 5a, $P < 0{\cdot}001$) and IgG3 (Fig. 5d, $P < 0{\cdot}001$). However, in both cases, the single transgenic control groups also showed similar differences indicating that this effect cannot be specifically attributed to the loss of PrP^C on FDC. Levels of IgG2a and IgG2b (Fig. 5b, $P > 0{\cdot}065$; Fig 5c, $P > 0{\cdot}09$) did not differ significantly between mice from each group. Although some differences in IgG subclass titres were observed between groups, none of these differences were specific to mice with PrP^C ablated on FDC.

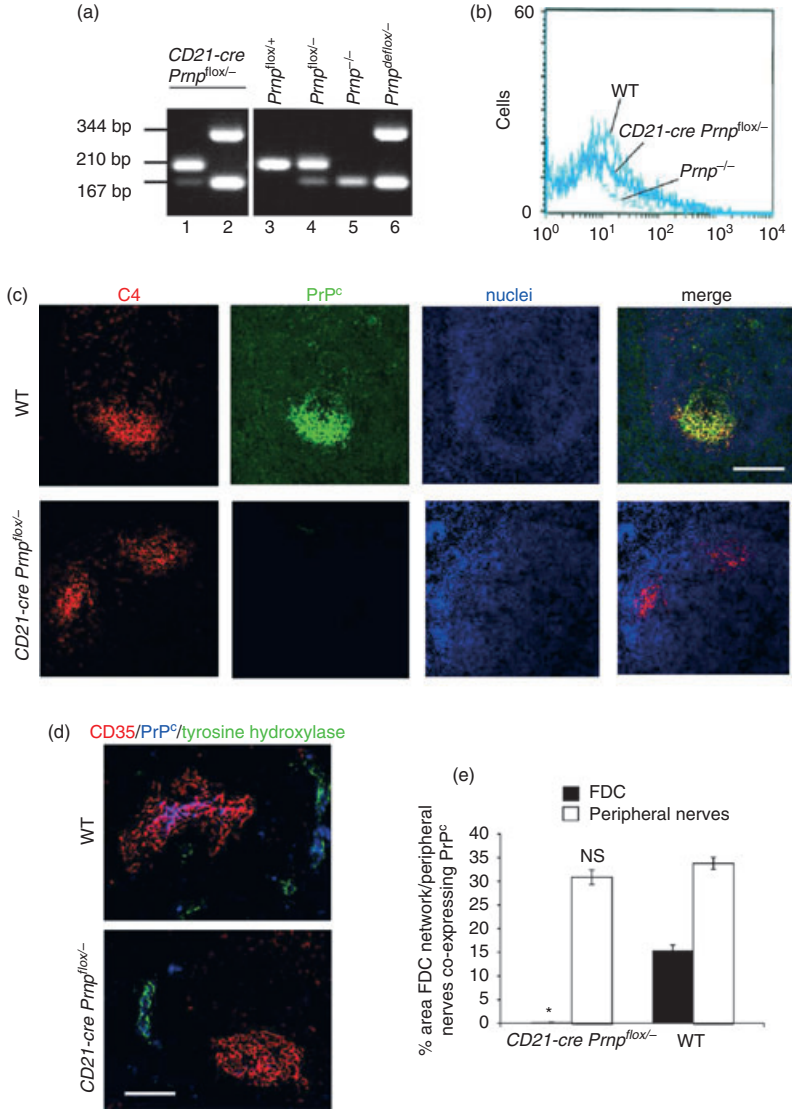

Figure 1. The cellular isomer of the prion protein (PrP^{C}) is ablated on the follicular dendritic cell (FDC) networks in spleens of *CD21-Cre Prnp$^{flox/-}$* mice. (a) PCR analysis of DNA isolated from the spleen and peripheral blood of bone marrow-reconstituted *CD21-Cre Prnp$^{flox/-}$* mice confirmed that efficient Cre-mediated DNA recombination and *Prnp* ablation (*Prnp^{deflox}*) was restricted to the FDC-containing stromal compartment of the spleen. In the spleens of *CD21-Cre Prnp$^{flox/-}$* mice, Cre-mediated DNA recombination (deletion or *de-flox*) of the *Prnp* gene had occurred as anticipated (lane 2, presence of 344 bp '*Prnp^{deflox}*' band). This indicated that PrP^{C} expression was ablated in the host-derived, FDC-containing stromal compartment of the spleen. In contrast, no evidence of Cre-mediated DNA recombination of the *Prnp* gene was detected in the peripheral blood of the *CD21-Cre Prnp$^{flox/-}$* mice (lane 1, presence of the 210 bp un-recombined '*Prnp^{flox}*' band and absence of the 344 bp '*Prnp^{deflox}*' band). This indicated that PrP^{C} expression by the Cre-deficient donor bone marrow-derived lymphocytes of these mice was not affected. (b) FACS analysis of PrP^{C} expression on splenic CD21^{+} B lymphocytes from *CD21-CrePrnp$^{flox/-}$* mice (thick line), wild-type (WT) mice (medium line) and PrP-deficient *Prnp$^{-/-}$* mice (fine broken line). Similar, low levels of PrP^{C} were detected on cells from WT and *CD21-Cre Prnp$^{flox/-}$* mice. *Prnp$^{-/-}$* mice were included as negative/background controls. (c) Immunohistochemical analysis of FDC (C4, red) and PrP^{C} (green) in spleens from WT mice demonstrates labelling of PrP^{C} present on the FDC networks. In *CD21-Cre Prnp$^{flox/-}$* mice, this labelling is absent, confirming the ablation of PrP^{C} on the FDC networks via *Cre*-mediated excision of the *Prnp* open reading frame. Scale bar 50 μm. (d) Immunohistochemical analysis of PrP^{C} expression (blue) by FDC (CD35^{+} cells; red) and sympathetic nerves (tyrosine hydroxylase^{+} cells, green) in the spleens of WT mice and *CD21-Cre Prnp$^{flox/-}$* mice. High levels of PrP^{C} were detected on FDC and nerves in the spleens of WT mice (upper panel). However, in spleens of *CD21-Cre Prnp$^{flox/-}$* mice the PrP^{C} ablation was restricted to FDC but not nerves (lower panel). Scale bar, 50 μm. (e) Morphometric analysis confirmed that the magnitude of the PrP^{C} expression co-localized upon the surfaces of FDC (closed bars) in the spleens of *CD21-Cre Prnp$^{flox/-}$* mice was substantially and significantly lower than that observed upon FDC from control mice ($*P < 1{\cdot}0 \times 10^{-22}$). In contrast, the magnitude of the PrP^{C} expression co-localized upon the surfaces tyrosine hydroxylase^{+} sympathetic nerves (open bars) in the spleens of *CD21-Cre Prnp$^{flox/-}$* mice was not significantly different when compared with controls (NS, $P = 0{\cdot}390$). Data derived from 48 images/group.

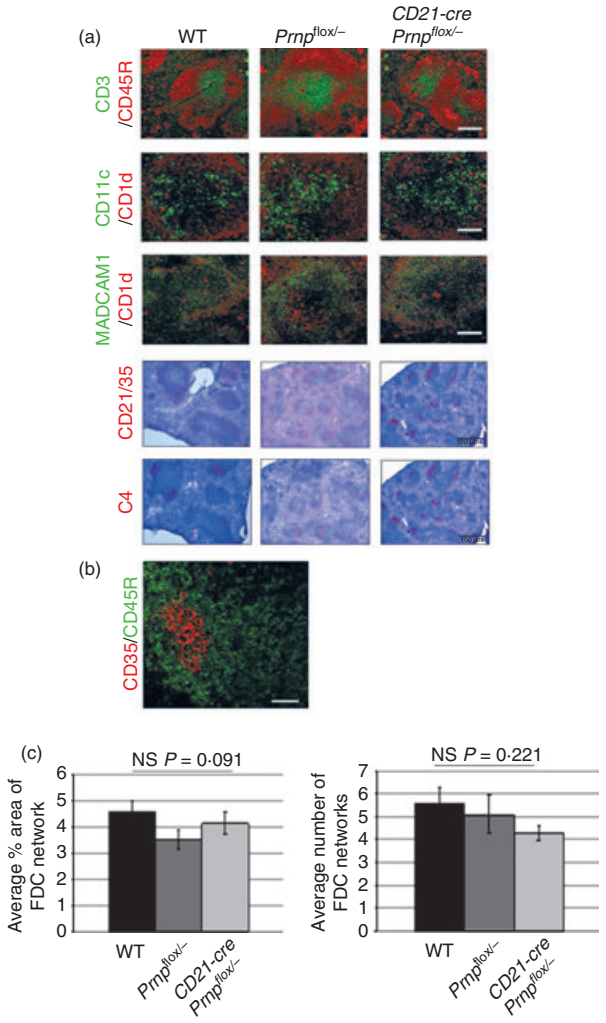

Figure 2. Ablation of the cellular isomer of the prion protein (PrP^C) specifically in follicular dendritic cells (FDC) has no effect on FDC status or lymphoid tissue microarchitecture. (a) Frozen spleens from mice with PrP^C ablated specifically in FDC (*CD21-Cre Prnp*$^{flox/-}$), were immunolabelled for FDC (C4, CD21/35), B-lymphocyte subsets (CD45R and CD1d), T lymphocytes (CD3), classical dendritic cells (CD11c) and marginal zone cells (MADCAM-1 and CD1d). Comparison of sections from PrP^C-ablated animals with *Prnp*$^{flox/flox}$ or wild-type (WT) controls showed no differences in the tissue microarchitecture or distribution of these cell subsets within the spleen. Scale bars on fluorescent images are 50 μm. Scale bars on light microscopy images are 500 μm and sections are counterstained with haematoxylin, blue. (b) Immunohistochemical analysis shows FDC ($CD35^+$ cells, red), in contrast to B cells (CD45R, green), specifically express high levels of CD35 in the spleen. (c) Morphometric analysis of FDC confirmed that there were no significant differences in the size or number of FDC networks in each group (FDC networks/field-of-view when viewed with the × 10 objective; n = 48 images analysed per group). Statistical analysis carried out using one-way analysis of variance. Data are representative of three independent experiments.

Taken together, these data show that ablation of PrP^C specifically on FDC does not impair their ability to induce a primary and secondary humoral immune response and has no impact on the affinity maturation of antigen-specific B lymphocytes in the follicle.

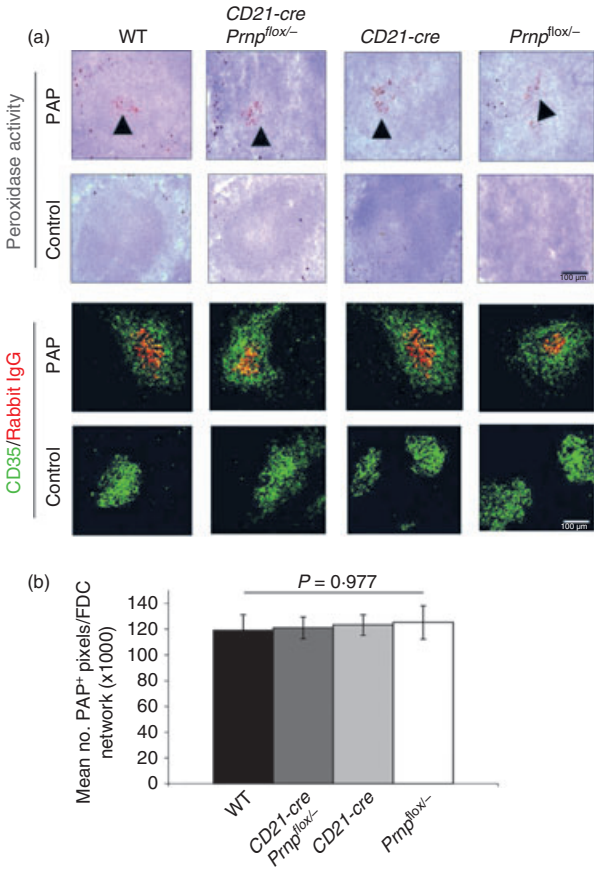

Figure 3. Ablation of the cellular isomer of the prion protein (PrP^C) specifically in follicular dendritic cells (FDC) has no effect on immune complex trapping. (a) Mice were passively immunized with rabbit peroxidase–anti-peroxidase (PAP) preformed immune complexes. Immune complex trapping by FDC was assessed 24 hr later by two methods. Peroxidase activity of PAP (▲) was localized to the follicles in all lines of mice. Immune complexes were then detected using anti-rabbit immunoglobulin conjugated to Alexa 555 (red) and double labelled for FDC ($CD35^+$ cells, green). No differences were observed between mouse lines, these data show that PrP^C ablation in FDC does not affect the ability of FDC to trap immune complexes. (b) No significant difference was observed in the mean number of PAP^+ pixels detected on each FDC network in spleens from mice from each group (n = 48 images analysed per group).

PrP^C ablation does not affect FDC maturation

After immunization, FDC induce the formation of the GC and up-regulate their expression of adhesion molecules and TLR4 to improve B-lymphocyte–FDC contact and direct the sub-class switching of B lymphocytes.[1,12,20] We therefore next determined whether PrP^C ablation affected the ability of the FDC to mature. Immunohistochemical analysis of spleens from immunized mice

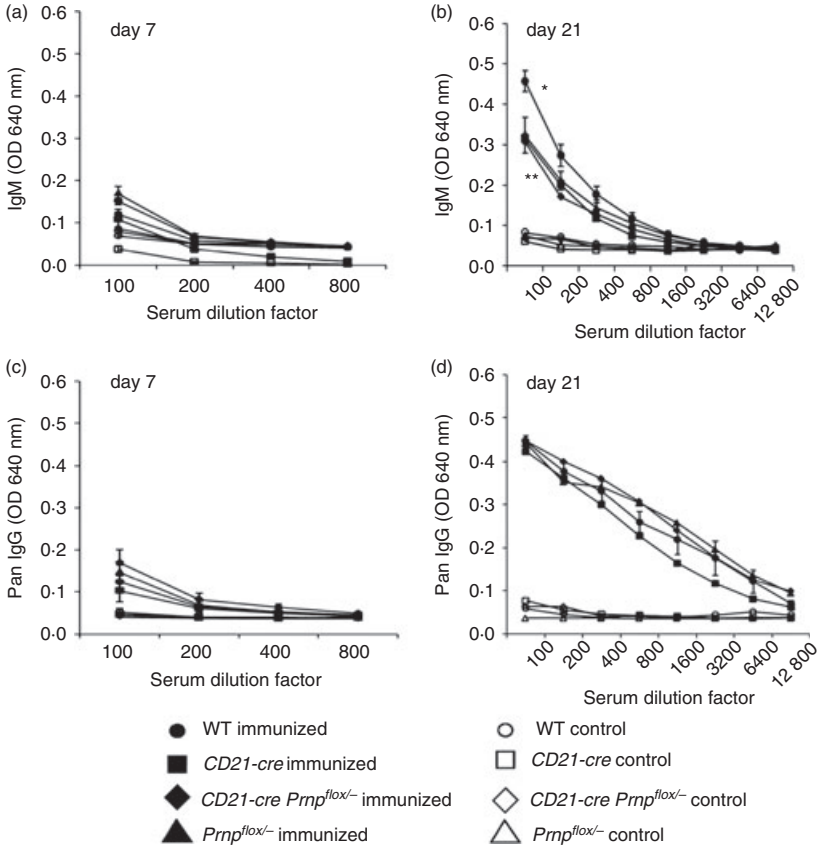

Figure 4. Ablation of the cellular isomer of the prion protein (PrP^C) specifically on follicular dendritic cells (FDC) has no effect on primary or secondary antibody responses. Mice were immunized on day 0 with 100 μl of 1 μg/μl dinitrophenyl–keyhole limpet haemocyanin (DNP-KLH) in alum intraperitoneally and given a boost with an equivalent intraperitoneal dose on day 14. ELISA was carried out on serum separated from blood taken on days 0, 7 and 21 to measure DNP-specific antibodies. Primary antibody response to the injected DNP-KLH was determined by measuring DNP-specific serum IgM (a) and total IgG (c) titres in serum taken at day 7 after immunization. Secondary antibody response was determined by measuring DNP-specific serum IgM (b) and total IgG (d) titres in serum taken at day 21. Serum from uninjected strain-matched controls was also analysed and day 0 serum was used to determine baseline titres. Bonferroni analysis was used to determine any significant differences between groups. At day 7, no significant differences could be found in IgM ($P = 1$; a) or total IgG ($P > 0{\cdot}07$; c) titres in serum from *CD21-Cre Prnp$^{flox/-}$* mice in comparison with wild-type (WT) and single transgenic controls. At day 21, IgM titres were significantly higher in WT controls in comparison to all other strains (*$P < 0{\cdot}001$; b) however no significant difference was observed between *CD21-Cre Prnp$^{flox/-}$* mice and single transgenic controls (**$P > 0{\cdot}625$; b). As lower titres of IgM were found in all transgenic lines, this difference in titre is not likely to be an effect of PrP^C ablation on FDC. No significant differences between any groups were observed in total IgG titres at day 21 ($P > 0{\cdot}07$; d).

showed that FDC-specific PrP^C ablation showed no difference in their expression of adhesion molecules (ICAM and VCAM) or TLR4 when compared with WT mice or the single transgenic controls (Fig. 6a). Furthermore, morphometric analysis suggested that there was no significant difference in the magnitude of the CD35-, TLR4-, ICAM1- and VCAM-specific immunostaining observed on the FDC networks of immunized WT and *CD21-Cre Prnp$^{flox/-}$* mice (Fig. 6b). These data suggest that PrP^C expression by FDC is dispensable for their maturation.

Discussion

The gene that encodes for PrP^C is highly conserved between mice and humans and is ubiquitously expressed in most cell types with expression of PrP^C being found in all vertebrates. This would imply that expression of PrP^C is directly or indirectly required for some vital cellular function. A definitive role for the high levels of PrP^C expressed on the FDC remains to be established. In this study, we assessed FDC function in mice with PrP^C ablation specifically restricted to FDC. The novelty of this study was that a cell-specific knockout of PrP^C using the *Cre-LoxP* system was used to determine an *in vivo*, physiologically relevant function of PrP^C expression on FDC. In the limited studies undertaken previously to assess the immune system in *Prnp$^{-/-}$* mice no evidence of immunodeficiency had been found.[60–63] However, studies so far have mainly involved *in vitro* challenge of *Prnp$^{-/-}$* cell populations or *in vivo* studies carried out in unchallenged

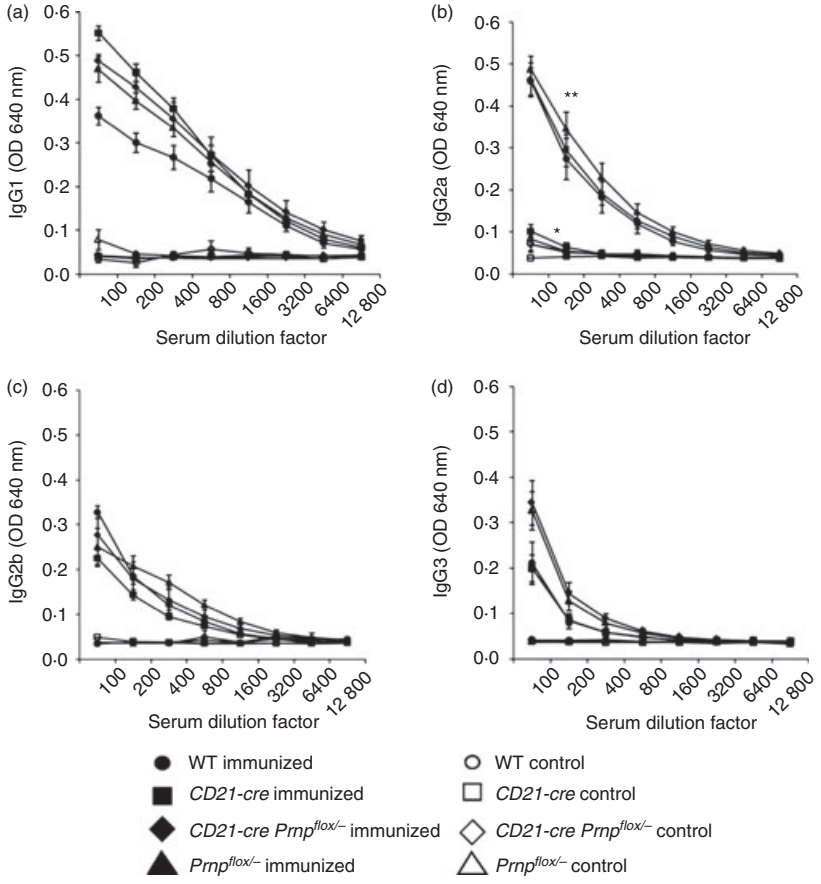

Figure 5. Ablation of the cellular isomer of the prion protein (PrP^C) specifically on follicular dendritic cells (FDC) has no effect on immunoglobulin class switching. Serum from mice immunized with dinitrophenyl–keyhole limpet haemocyanin (DNP-KLH) was also analysed for titres of IgG subclasses to assess the level of class switching occurring in mice with PrP^C ablated on FDC in comparison to control groups. Serum was analysed at days 0, 7 and 21 but as early titres were low, only data from day 21 are shown. Titres of IgG1 in all transgenic lines were significantly higher than that measured in wild-type (WT) controls ($P < 0{\cdot}001$; a). *CD21-Cre* single transgenic mice have significantly lower titres of IgG2a in comparison to other groups (*$P < 0{\cdot}001$; b), however titres in *CD21-Cre* $Prnp^{flox/-}$ mice are not significantly different to those in WT or $Prnp^{flox/-}$ lines (**$P > 0{\cdot}065$; b). No significant differences in titre of IgG2b was observed between groups ($P > 0{\cdot}09$; c). *CD21-Cre* $Prnp^{flox/-}$ mice have significantly higher titres of IgG3 in comparison to WT and single transgenic *CD21-Cre* controls (*$P < 0{\cdot}001$; d), however $Prnp^{flox/-}$ mice have similar titres (**$P = 1$; d). Although there are some slight differences in IgG subclass titres between groups, no differences are specific to mice with PrP^C ablated in FDC and therefore ablation of PrP^C in FDC does not appear to have any specific effects on immunoglobulin class switching after immunization.

mice kept in pathogen-free conditions. It remains possible that under these steady-state conditions a functional role for PrP^C within the immune system is hard to determine. For this reason, analysis of the effects of PrP^C ablation specifically on FDC were carried out in *in vivo* models under both normal homeostatic conditions and following immunization.

In these studies, no effects on the development of the lymphoid follicle were found in mice with PrP^C-ablated FDC. Furthermore, these mice had no impairments in their ability to trap immune complexes on their surface and no defects in their ability to produce antigen-specific antibodies or undergo affinity maturation. These data are consistent with previous studies showing that $Prnp^{-/-}$ mice are able to elicit effective antigen-specific antibody responses following immunization with PrP.[30,64,65] The FDC were also able to mature functionally in the GC with no observable impairments. Together these data show that PrP^C expression on FDC is dispensable for their functional maturation and ability to maintain antigen-specific antibody production and affinity maturation in the GC.

One hypothesized function of PrP^C is in the formation of intercellular gap junctions. A loss of PrP^C has been found to weaken gap junctions in the intestinal epithelial cell layer resulting in increased permeability of the mucosa.[66] FDC networks are reported to be connected to each other and to surrounding B lymphocytes via gap junctions.[67] In the analysis carried out in this study the development of FDC networks and the surrounding

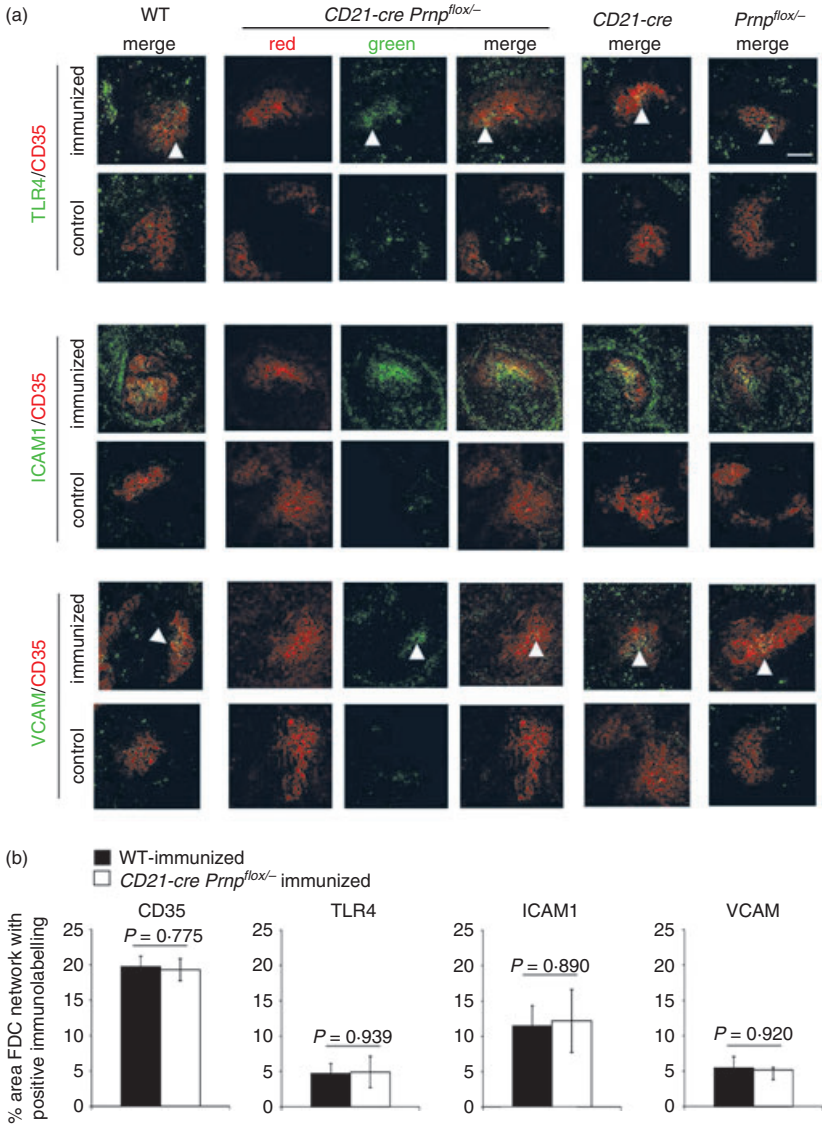

Figure 6. Ablation of cellular isomer of the prion protein (PrP^{C}) specifically on follicular dendritic cells (FDC has no effect on FDC maturation. (a) Spleens from *CD21-Cre Prnp$^{flox/-}$* mice with PrP^{C} ablated specifically in FDC that had been immunized with dinitrophenyl–keyhole limpet haemocyanin (DNP-KLH), were immunolabelled for FDC (CD35), and various markers which are up-regulated on FDC during an active GC response [Toll-like receptor 4 (TLR4), intercellular adhesion molecule (ICAM) and vascular cell adhesion molecule (VCAM)]. Comparison of sections from PrP^{C}-ablated animals with *CD21-Cre*, *Prnp$^{flox/-}$* or wild-type (WT) controls showed no differences in the expression of these markers on FDC after immunization. Scale bar 100 μm. These data show that ablation of PrP^{C} on FDC has no effect on the ability of the FDC to mature and become activated during a germinal centre response to injected antigen. (b) Morphometric analysis suggested there were no significant differences in the magnitude of the CD35-, TLR4-, ICAM1- and VCAM-specific immunostaining observed on the FDC networks of immunized WT and *CD21-Cre Prnp$^{flox/-}$* mice.

B-lymphocyte follicle appeared to be normal, with no abnormalities in GC formation or downstream antibody responses. However, as the gap junctions themselves were not specifically analysed, the possibility still remains that they are weakened in mice with PrP^{C} ablated in FDC. Another suggested role for PrP^{C} is protection against oxidative stress. So it is plausible that a loss of PrP^{C} may only show phenotypic characteristics in aged mice or conditions of oxidative stress. Furthermore, ultra-structural studies of PrP-deficient FDC in comparison to WT counterparts may be required to provide indications as to the precise function of PrP^{C} on FDC.

Many studies investigating the function of PrP^{C} in both the CNS and the immune system in various *Prnp$^{-/-}$* mouse lines have similarly struggled to find a definitive functional role for PrP^{C} expression. Although several functions have been proposed for PrP^{C} within the CNS, many of these reported findings such as synaptic transmission, have little bearing on why cells of the immune system, and more specifically FDC, should express such high levels of this protein. Within the immune system, PrP^{C} has been reported to have several potentially conflicting functions. In T lymphocytes, PrP^{C} is found within the immunological synapse and co-localizes with the T-lymphocyte receptor (TCR) after TCR cross-linking. Cross-linking of this PrP^{C} on T lymphocytes using anti-PrP antibodies has been shown to stimulate T lymphocytes as measured via calcium flux.[68] Others, in contrast, have suggested that anti-PrP antibodies block T-lymphocyte activation by concanavalin A, anti-TCR and MHC peptide.[63,69,70] These apparently contradicting data highlight the many difficulties encountered in determining the function of PrP^{C} in the immune system.

In conclusion, data presented here show that PrP^{C} expression is dispensable for the functional maturation of

FDC and their ability to maintain antigen-specific antibody responses and affinity maturation. As a consequence, the precise role of PrP^C expression on the FDC remains elusive. Further studies are necessary to understand the biology of this highly conserved cellular protein both in the context of normal immune function and prion disease pathogenesis to better our knowledge of these processes.

Acknowledgements

We thank Barry Bradford, Bob Fleming, Nadia Tuzi, Irene McConnell, Fraser Laing, Simon Cumming and the Pathology Services Group (University of Edinburgh, UK) for helpful discussion and excellent technical support; Nathalie Uyttersprot (current address, Artemis Pharmaceuticals GmbH, Germany), Ari Waisman (Johannes Gutenberg University of Mainz, Germany) and Klaus Rajewsky (Harvard Medical School, Massachusettes, USA) for supplying the *CD21-cre* mice; Jean Manson (University of Edinburgh, UK) for providing the $Prnp^{-/-}$ and $PrP^{flox/flox}$ mouse lines; and Herbert Baybutt (University of Edinburgh, UK) for help with statistical analyses using SPSS software. This research was supported by project (Grant numbers BB/526741-1 and BBS/E/R/00001813) and institute strategic grant funding from the BBSRC.

Disclosures

The authors declare no financial or commercial conflict of interests.

References

1 Heinen E, Bosseloir A, Bouzahzah F. Follicular dendritic cells: origin and function. *Curr Top Microbiol Immunol* 1995; **201**:15–47.
2 Wang X, Cho B, Suzuki K, Xu Y, Green JA, An J, Cyster JG. Follicular dendritic cells help establish follicle identity and promote B cell retention in germinal centers. *J Exp Med* 2011; **208**:2497–510.
3 Kapasi ZF, Burton GF, Shultz LD, Tew JG, Szakal AK. Induction of functional follicular dendritic cell development in severe combined immunodeficiency mice. Influence of B and T cells. *J Immunol* 1993; **150**:2648–58.
4 Kapasi ZF, Qin D, Kerr WG, Kosco-Vilbois MH, Shultz LD, Tew JG, Szakal AK. Follicular dendritic cell (FDC) precursors in primary lymphoid tissues. *J Immunol* 1998; **160**:1078–84.
5 Balogh P, Aydar Y, Tew JG, Szakal AK. Ontogeny of the follicular dendritic cell phenotype and function in the postnatal murine spleen. *Cell Immunol* 2001; **214**:45–53.
6 Chaplin DD, Fu YX. Cytokine regulation of secondary lymphoid organ development. *Curr Opin Immunol* 1998; **10**:289–97.
7 Victoratos P, Lagnel J, Tzima S, Alimzhanov MB, Rajewsky K, Pasparakis M, Kollias G. FDC-specific functions of p55TNFR and IKK2 in the development of FDC networks and of antibody responses. *Immunity* 2006; **24**:65–77.
8 Krautler NJ, Kana V, Kranich J, *et al.* Follicular dendritic cells emerge from ubiquitous perivascular precursors. *Cell* 2012; **150**:194–206.
9 Qin D, Wu J, Vora KA, Ravetch JV, Szakal AK, Manser T, Tew JG. Fcγ receptor IIB on follicular dendritic cells regulates the B cell recall response. *J Immunol* 2000; **164**:6268–75.
10 Gray D, Skarvall H. B-cell memory is short-lived in the absence of antigen. *Nature* 1988; **336**:70–3.
11 Gray D, Kosco MH, Stockinger B. Novel pathways of antigen presentation for the maintenance of memory. *Int Immunol* 1991; **3**:141–8.
12 Kosco MH, Pflugfelder E, Gray D. Follicular dendritic cell-dependent adhesion and proliferation of B cells *in vitro*. *J Immunol* 1992; **148**:2331–9.
13 Suzuki K, Grigorova I, Phan TG, Kelly LM, Cyster JG. Visualizing B cell capture of cognate antigen from follicular dendritic cells. *J Exp Med* 2009; **206**:1485–93.
14 Roozendaal R, Carroll MC. Complement receptors CD21 and CD35 in humoral immunity. *Immunol Rev* 2007; **219**:157–66.
15 Nielsen CH, Fischer EM, Leslie RGQ. The role of complement in the acquired immune response. *Immunology* 2000; **100**:4–12.
16 Videm V, Albrigtsen M. Soluble ICAM-1 and VCAM-1 as markers of endothelial activation. *Scand J Immunol* 2008; **67**:523–31.
17 Kosco-Vilbois MH, Bonnefoy JY, Chvatchko Y. The physiology of murine germinal center reactions. *Immunol Rev* 1997; **156**:127–36.
18 Kopf M, Herren S, Wiles MV, Pepys MB, Kosco-Vilbois MH. Interleukin 6 influences germinal center development and antibody production via a contribution of C3 complement component. *J Exp Med* 1998; **188**:1895–906.
19 Hase H, Kanno Y, Kojima M, *et al.* BAFF/BLys can potentiate B-cell selection with the B-cel coreceptor complex. *Blood* 2004; **103**:2257–65.
20 Suzuki K, Maruya M, Kawamoto S, Sitnik K, Kitamura H, Agace WW, Fagarasan S. The sensing of environmental stimuli by follicular dendritic cells promotes immunoglobulin A generation in the gut. *Immunity* 2010; **33**:71–83.
21 Kranich J, Krautler NJ, Heinen E, *et al.* Follicular dendritic cells control engulfment of apoptotic bodies by secreting Mfge8. *J Exp Med* 2008; **205**:1293–302.
22 Ho J, Moir S, Kulik L, *et al.* Role for CD21 in the establishment of an extracellular HIV reservoir in lymphoid tissues. *J Immunol* 2007; **178**:6968–74.
23 Manson JC, Clarke AR, Hooper ML, Aitchison L, McConnell I, Hope J. 129/Ola mice carrying a null mutation in PrP that abolishes mRNA production are developmentally normal. *Mol Neurobiol* 1994; **8**:121–7.
24 Brown KL, Stewart K, Ritchie DL, Mabbott NA, Williams A, Fraser H, Morrison WI, Bruce ME. Scrapie replication in lymphoid tissues depends on prion protein-expressing follicular dendritic cells. *Nat Med* 1999; **5**:1308–12.
25 McCulloch L, Brown KL, Bradford BM, Hopkins J, Bailey M, Rajewsky K, Manson JC, Mabbott NA. Follicular dendritic cell-specific prion protein (PrP^C) expression alone is sufficient to sustain prion infection in the spleen. *PLoS Pathog* 2011; **7**:e1002402.
26 Caughey B, Race RE, Chesebro B. Detection of prion protein mRNA in normal and scrapie-infected tissues and cell lines. *J Gen Virol* 1988; **69**:711–6.
27 Kretzschmar HA, Prusiner SB, Stowring LE, deArmond SJ. Scrapie prion proteins are synthesised in neurones. *Am J Pathol* 1986; **122**:1–5.
28 Brown HR, Goller NL, Rudelli RD, Mertz GS, Wolfe GC, Wisniewski HM, Robakis NK. The mRNA encoding the scrapie agent protein is present in a variety of non-neuronal cells. *Acta Neuropathol* 1990; **80**:1–6.
29 Ford MJ, Burton LJ, Morris RJ, Hall SM. Selective expression of prion protein in peripheral tissues of the adult mouse. *Neuroscience* 2002; **113**:177–92.
30 Prusiner SB, Groth D, Serban A, *et al.* Ablation of the prion protein (PrP) gene in mice prevents scrapie and facilitates production of anti-PrP antibodies. *Proc Natl Acad Sci USA* 1993; **90**:10608–12.
31 Lasmézas CI. Putative functions of PrP^c. *Br Med Bull* 2003; **66**:61–70.
32 Prusiner SB, Scott MR, DeArmond SJ, Cohen FE. Prion protein biology. *Cell* 1998; **93**:337–48.
33 Tobler I, Gaus SE, Deboer T, *et al.* Altered circadian activity rhythms and sleep in mice devoid of prion protein. *Nature* 1996; **380**:639–42.
34 Collinge J, Whittington MA, Sidle KCL, Smith CJ, Palmer MS, Clarke AR, Jefferys JGR. Prion protein is necessary for normal synaptic function. *Nature* 1994; **370**:295–7.
35 Nico PBC, de-Paris F, Vinade ER, *et al.* Altered behavioural response to acute stress in mice lacking cellular prion protein. *Behav Brain Res* 2005; **162**:173–81.
36 Coitinho AS, Roesler R, Martins VR, Brentani RR, Izquierdo I. Cellular prion protein ablation impairs behavior as a function of age. *NeuroReport* 2003; **14**:1375–9.
37 Walz R, Amaral OB, Rockenbach IC, Roesler R, Izquierdo I, Cavalheiro EA, Martins VR, Brentani RR. Increased sensitivity to seizures in mice lacking cellular prion protein. *Epilepsia* 1999; **40**:1679–82.
38 Mouillet-Richard S, Ermonval M, Chebassier C, Laplanche JL, Lehmann S, Launay JM, Kellermann O. Signal transduction through prion protein. *Science* 2000; **289**:1925–8.
39 Spielhaupter C, Schätzl HM. PrP^C directly interacts with proteins involved in signaling pathways. *J Biol Chem* 2001; **276**:44604–12.
40 Paitel E, Alves da Costa C, Vilette D, Grassi J, Checler F. Overexpression of PrPc triggers caspase 3 activation: potentiation by proteasome inhibitors and blockade by anti-PrP antibodies. *J Neurochem* 2002; **83**:1208–14.
41 Kurschner C, Morgan JI. The cellular prion protein (PrP) selectively binds to Bcl-2 in the yeast two-hybrid system. *Mol Brain Res* 1995; **30**:165–8.
42 Bounhar Y, Zhang Y, Goodyer CG, LeBlanc A. Prion protein protects human neurons against Bax-mediated apoptosis. *J Biol Chem* 2001; **276**:39145–9.
43 Mitteregger G, Vosko M, Krebs B, Xiang W, Kohlmannsperger V, Nolting S, Hamann GF, Kretzschmar HA. The role of the octarepeat region in neuroprotective function of the cellular prion protein. *Brain Pathol* 2007; **17**:174–83.

44 Aude-Garcia C, Villiers C, Candéias S, Garrel C, Bertrand C, Collin V, Marche P, Jouvin-Marche E. Enhanced susceptibility of T lymphocytes to oxidative stress in the absence of the cellular prion protein. *Cell Mol Life Sci* 2011; **68**:687–96.

45 Kraus M, Alimzhanov MB, Rajewsky N, Rajewsky K. Survival of resting mature B lymphocytes depends on BCR signaling via the Igα/β heterodimer. *Cell* 2004; **117**:787–800.

46 Tuzi NL, Clarke AR, Bradford B, Aitchison L, Thomson V, Manson JC. Cre-loxP mediated control of PrP to study transmissible spongiform encephalopathy diseases. *Genesis* 2004; **40**:1–6.

47 Manson JC, Clarke AR, McBride PA, McConnell I, Hope J. PrP gene dosage determines the timing but not the final intensity or distribution of lesions in scrapie pathology. *Neurodegeneration* 1994; **3**:331–40.

48 Farquhar CF, Somerville RA, Ritchie LA. Post-mortem immunodiagnosis of scrapie and bovine spongiform encephalopathy. *J Virol Methods* 1989; **24**:215–21.

49 Inman CF, Rees LEN, Barker E, Haverson K, Stokes CR, Bailey M. Validation of computer-assisted, pixel-based analysis of multiple-colour immunofluorescence histology. *J Immunol Methods* 2005; **302**:156–67.

50 Liu Y-J, Xu J, de Bouteiller O, *et al.* Follicular dendritic cells specifically express the long CR2/CD21 isoform. *J Exp Med* 1997; **185**:165–70.

51 Takahashi K, Kozono Y, Waldschmidt TJ, Berthiaume D, Quigg RJ, Baron A, Holers VM. Mouse complement receptors type 1 (CR1;CD35) and type 2 (CR2;CD21): expression on normal B cell subpopulations and decreased levels during the development of autoimmunity in MRL/lpr mice. *J Immunol* 1997; **159**:1557–69.

52 Tsoukas CD, Lambris JD. Expression of CR2/EBV receptors on human thymocytes detected by monoclonal antibodies. *Eur J Immunol* 1988; **18**:1299–302.

53 June RA, Landay AL, Stefanik K, Lint TF, Spear GT. Phenotypic analysis of complement receptor 2^+ T lymphocytes: reduced expression on $CD4^+$ cells in HIV-infected persons. *Immunology* 1992; **75**:59–65.

54 Sixbey J, Lemon S, Pagano J. A second site for Epstein–Barr virus shedding: the uterine cervix. *Lancet* 1986; **328**:1122–4.

55 Andrasfalvy M, Prechl J, Hardy T, Erdei A, Bajtay Z. Mucosal type mast cells express complement receptor type 2 (CD21). *Immunol Lett* 2002; **82**:29–34.

56 Kosco-Vilbois MH. Are follicular dendritic cells really good for nothing? *Nat Rev Immunol* 2003; **3**:764–9.

57 Oda M, Uchiyama S, Noda M, *et al.* Effects of antibody affinity and antigen valence on molecular forms of immune complexes. *Mol Immunol* 2009; **47**:357–64.

58 Keşmir C, De Boer RJ. A spatial model of germinal center reactions: cellular adhesion based sorting of B cells results in efficient affinity maturation. *J Theor Biol* 2003; **222**:9–22.

59 Vora KA, Ravetch JV, Manser T. Amplified follicular immune complex deposition in mice lacking the Fc receptor γ-chain does not alter maturation of the B cell response. *J Immunol* 1997; **159**:2116–24.

60 Genoud N, Behrens A, Miele G, Robay D, Heppner FL, Freigang S, Aguzzi A. Disruption of Doppel prevents neurodegeneration in mice with extensive Prnp deletions. *Proc Natl Acad Sci USA* 2004; **101**:4198–203.

61 Bueler H, Fischer M, Lang Y, *et al.* Normal development and behaviour of mice lacking the neuronal cell-surface PrP protein. *Nature* 1992; **356**:577–82.

62 Ballerini C, Gourdain P, Bachy V, *et al.* Functional implication of cellular prion protein in antigen-driven interactions between T cells and dendritic cells. *J Immunol* 2006; **176**:7254–62.

63 Kubosaki A, Yusa S, Nasu Y, *et al.* Distribution of cellular isoform of prion protein in T lymphocytes and bone marrow, analyzed by wild-type and prion protein gene-deficient mice. *Biochem Biophys Res Commun* 2001; **282**:103–7.

64 Williamson RA, Peretz D, Smorodinsky N, *et al.* Circumventing tolerance to generate autologous monoclonal antibodies to the prion protein. *Proc Natl Acad Sci USA* 1996; **93**:7279–82.

65 Khalili-Shirazi A, Quaratino S, Londei M, *et al.* Protein conformation significantly influences immune responses to prion protein. *J Immunol* 2005; **174**:3256–63.

66 Petit CSV, Barreau F, Besnier L, *et al.* Requirement of cellular prion protein for intestinal barrier function and mislocalization in patients with inflammatory bowel disease. *Gastroenterology* 2012; **143**:122–32.

67 Krenacs T, van Dartel M, Lindhout E, Rosendaal M. Direct cell/cell communication in the lymphoid germinal center: connexin43 gap junctions functionally couple follicular dendritic cells to each other and to B lymphocytes. *Eur J Immunol* 1997; **27**:1489–97.

68 Stuermer CAO, Langhorst MF, Wiechers MF, Legler DF, Von Hanwehr SH, Guse AH, Plattner H. PrPc capping in T cells promotes its association with the lipid raft proteins reggie-1 and reggie-2 and leads to signal transduction. *FASEB J* 2004; **18**:1731–3.

69 Cashman NR, Loertscher R, Nalbantoglu J, Shaw I, Kascsak RJ, Bolton DC, Bendheim PE. Cellular isoform of the scrapie agent protein participates in lymphocyte activation. *Cell* 1990; **61**:185–92.

70 Li R, Liu D, Zanusso G, *et al.* The expression and potential function of cellular prion protein in human lymphocytes. *Cell Immunol* 2001; **207**:49–58.